Letters in Applied NanoBioScience
Open-Access Journal (ISSN: 2284-6808)

Article
Volume 12, Issue 2, 2023, 35
https://doi.org/10.33263/LIANBS122.035

Development of Antimicrobial Dressings by the Action of Silver Nanoparticles Based on Green Nanotechnology

Julia Santana [1], Sérgio Antunes [1,2], Raquel Bonelli [2], Bianca Backx [1,*]

[1] Numpex-Bio, Universidade Federal do Rio de Janeiro, Campus Duque de Caxias, Brazil;
[2] Instituto de Microbiologia Professor Paulo de Goes, Universidade Federal do Rio de Janeiro, Rio de Janeiro, Brazil;
* Correspondence biapizzorno@caxias.ufrj.br (B.B.), biapizzorno@gmail.com (B.B.);

Scopus Author ID 56455326500

Received: 22.11.2021; Accepted: 4.01.2022; Published: 14.03.2022

Abstract: Alternatives have been investigated to reduce the environmental impact of waste emitted in the health field. The replacement of conventional polymers with biodegradable polymers in hospital dressings is one. Corn starch is a biopolymer, biodegradable, with skin regenerating properties. Glycerol is a by-product of biodiesel synthesis, and when polymerized, it becomes polyglycerol, a polymer with plasticizing characteristics. Therefore, a polymer blend is shaped based on another promising natural compound: *Euterpe oleracea* extract. This extract has fundamental antioxidant properties for the efficient synthesis and dispersion of silver nanoparticles. These nanostructures have, among many characteristics, antimicrobial properties. This article reports the development of a polymer blend, based on açaí fruit extract and dispersion of AgNPs, for the production of biodegradable filmogenic dressings that do not require the use of glue. It was observed that the *Euterpe oleracea* extract is an efficient reducer and stabilizer of AgNPs. The antimicrobial sensitivity test, the antimicrobial efficiency of the polymeric blends, and the AgNPs in the *S. aureus* ATCC 25923 and *E. coli* ATCC 25922 strains were confirmed.

Keywords: silver nanoparticles; starch-based biodegradable films; mixtures of polymers.

1. Introduction

Millions of synthetic plastic films are produced and disposed of in the environment without control. An alternative to synthetic plastics that last in the environment is the use of biodegradable polymers made from renewable sources [1,2].

The production of biofilms is based on the formulation of a solution where the biopolymers are dispersed or solubilized in a solvent, such as water, ethanol, or organic acids; besides the insertion of additives or not, such as plasticizers or alloying agents, which after heating end up forming a filmogenic dispersion [3–5].

To improve some properties of these films and upgrade mechanical, physical, and chemical properties, polymer blends are produced, which is the physical mixture of two or more polymers, with the main objective of increasing the physical and chemical properties of the material [6–10].

Polysaccharides such as starch and cellulose make up most of the biopolymers found in nature. Starch is organized in a conformation where layers of amylopectin and amylose (glucose polymers) are deposited around the hilum, a central point. The accumulation causes an increase in the structure and the formation of semicrystalline granules, formed by long chains of glucose interconnected and rolled up together. Amylopectin is a highly branched

molecule, while amylose has a linear conformation. The proportion between amylose and amylopectin is related to its botanical source, varying and, for this reason, giving specific characteristics for each starch paste. The starch structure, its physical organization inside the granule, and its functionalities are correlated with these two macromolecules [11]. The crystalline regions of starch provide resistance to enzymatic and chemical attacks, maintain their granular structure and behavior in the presence of water, and the grain's interior has a high degree of supramolecular organization [12,13]. Polymerization of glycerol (generating polyglycerol) in synergy with corn starch produces polymeric blends.

There is an advanced search for non-toxic and natural solutions with antimicrobial activity. The growing need for ecologically correct synthesis pathways has increased interest in studies on green nanoparticle synthesis [14–17].

The green synthesis of silver nanoparticles through plant extracts is based on redox between the extractive medium's compounds and the silver ion arising from the silver nitrate that undergoes ionic dissociation in the dispersive medium. In this way, the reduction of silver to the fundamental state occurs. Then, the nucleation and growth process begins, producing the AgNPs stabilized by the biomolecules present in the established colloidal matrix [18].

That said, in the present study for the stabilization of AgNPs, *Euterpe oleracea* (açaí) extract was used as a dispersive medium for AgNPs and production of blends with biodegradable polymers. The study of the extract was carried out from the peel and pulp of ripe fruits and green fruits to formulate biodegradable films with antimicrobial activity for a future application in the treatment of burn injuries and also to be used in hospital environments since the proposed dressing would not require the use of glue [19–23].

2. Materials and Methods

2.1. Obtaining raw materials.

The fruits of *Euterpe Oleracea* were obtained from family plantations in Pará, located in the North of Brazil, with an equatorial climate and at latitude 01º27'21" south and longitude 48º30'16" west, and farms in the interior of Rio de Janeiro, located in the southeastern region of the country, with a tropical climate and at latitude 22º54'23" south and longitude 43º10'21" west. No use of pesticides and fertilizers. Corn starch is produced by Yoki Alimentos S / A [24,25].

2.2. Production of Euterpe oleracea extract.

The methodology consisted of crushing the skins and pulps, only changing the degree of maturation for green and senescent seeds. The procedure for obtaining *Euterpe oleracea* extract was carried out using about 40 grams of *E. oleracea* seeds, rinsed with deionized water, and taken for heating by immersion methodology in 200 mL of deionized water up to 100 ºC per approximately 20 minutes. After this stage, the seeds were crushed. The filtration step was carried out using a paper filter weighing 80 g/m², and when completed, the extract was kept in an amber flask at room temperature for varying times [26,27].

2.3. Characterization of the extract by UV-Vis spectrophotometry.

The spectrophotometer used was The Thermo Evolution 60S. The extract analysis was performed using the scanning technique between the 200 nm and 800 nm ranges. Analyzes of

green seed and senescent seeds were made, the latter having a more explicit reading on UV-Vis. The cuvette used was quartz, and the white (baseline) of the solutions was deionized water. All analyzes were repeated in duplicates [28,29].

2.4. Synthesis of AgNPs through green synthesis methodology.

0.0169 g of $AgNO_3$ were weighed into 10 ml of solution, the concentration of 0.01 Mol / L (2.5 ml of concentrated extract to 7.5 ml of deionized H_2O). This solution was subjected to heating and stirring until it reached a temperature of 60 ºC. Only after reaching the temperature, the aqueous silver nitrate solution was added. Warm-ups were performed for 25 seconds, 30 seconds, 35 seconds, and 45 seconds. Thus, the time established for the methodology was 25 seconds of warm-up. Both tests were performed in duplicates [30,31].

2.5. Characterization of AgNPs by UV-Vis spectrophotometry.

The Thermo Evolution 60S spectrophotometer was used. This technique was used to analyze the formation and stability of AgNPs. In addition, these nanoparticles were also evaluated by scanning in the 200 nm to 800 nm range. The blank (baseline) used to analyze these solutions was *Euterpe oleracea* extract diluted to 25% v / v. All analyses were performed in duplicates [32].

2.6. Production of biodegradable film from the polymer blend.

For the biodegradable film production, the extract used was the one produced with ripe fruits, together with 5 g of cornstarch, in addition to the mass of 1.30 g of glycerol and 10 µL of polymerized glycerol (polyglycerol). Thus, the biopolymer interacts with polyglycerol to produce the blend. From this, the synthesis route of the polymer blend uses a solution of *Euterpe oleracea* extract with the AgNPs previously synthesized, where the proportion used in 30 mL of concentrated extract, heated by 90°C for approximately 10 minutes, 60 mL of deionized water, and 10 mL of a solution containing AgNPs produced via green synthesis, as demonstrated in item 4 of this materials and methods [33].

2.7. Analysis of the film's morphological viability.

For the analysis of morphological viability, 10 µL of different solutions were used to simulate environments similar to those of the application of the dressing to verify the structure of the film after being subjected to these conditions. The tested solutions were: deionized water, ortho-boric acid-H_3BO_3 (boric acid water), hydrogen peroxide-H_2O_2 (10 volumes commercial hydrogen peroxide), CH_3CH_2OH (70% ethyl alcohol), NaCl (saline), CH_3COOH 0.1 M (acetic acid) – (pH = 1) (acid) and $Mg(OH)_2$ (magnesium hydroxide) – (pH = 10) (basic). The samples used in the morphological viability test were cut manually around 1cm x 1cm (figure 6 (4)). Tests were performed in duplicates [34,35].

2.8. Characterization of the biodegradable film with AgNPs by optical microscopy, scanning electron microscopy, and dispersive energy spectroscopy (EDS).

The films were preliminarily analyzed by the Nikon Eclipse E200 optical microscope at 10x magnification to analyze corn starch's structure and a possible characterization of the AgNPs. In addition, the films were analyzed to observe possible structural changes.

To analyze the presence, dispersion, and behavior of AgNPs, characterizations were made using the scanning electron microscope VEGA 3 LMU; manufacturer Tescan; operating between 15 and 20kV. Before preparing samples, the seven metal bases were washed with acetone to remove grease, oil, particles, dust, or other contaminants. Then, EDS analysis was performed using the detector coupled to the scanning electron microscope mentioned above [36].

2.9. Characterization of AgNPs presents in polymer blends after chemical surface treatment by characteristic X-ray mapping.

To ascertain whether the treatment with a chemical surface attack (item 7) would preserve or eliminate the AgNPs in the blends and assess whether the AgNPs would remain dispersed in the material, elementary characterization mappings were carried out through the EDS. The technique's objective is to reveal the dispersion of the chemical elements on the surface of the films, which consists of an additional analysis made by the scanning electron microscope VEGA 3 LMU from the manufacturer Tescan [37,38].

2.10. Antimicrobial sensitivity test.

In the qualitative antimicrobial sensitivity test, the bacterial strains *S. aureus* ATCC 25923 and *E. coli* ATCC 25922, were incubated for 24h at 37ºC in Tryptic Soy Agar (Difco (R)) and, after that, resuspended in NaCl solution (0,85%) up to the 0.5 MacFarland turbidity range. Then, they were sown on Mueller Hinton Agar (Difco®) in a confluent manner, under conditions similar to those used in diffusion disk antibiograms (EUCAST, 2021). The AgNPs solutions were sterilized by filtration at 0.22 μm (Micropore®). The susceptibility test was carried out by diffusion using five strategies: (I) applying 20 μL of the AgNPs solutions (in their original concentration and diluted 1:10) in sterile filter paper discs (H and I); (II) disk of the dry polymer blend containing AgNPs incorporated during its synthesis (F); (III) dry polymer blend blended with H_2O + $AgNO_3$ solution and a sterile disc containing H_2O + $AgNO_3$ solution (D and G); (IV) sterile disk without solution and another with pure *Euterpe Oleracea* extract (B and E) and (V) water-based synthetic blend and one containing pure *Euterpe Oleracea* extract (A and C). The disks were 0.6 cm in diameter in both cases, with case preparation (i) performed directly on the inoculated culture medium. The dry polymer blend disc, composed of silver nitrate, was used for the positive control during the blend synthesis. The dry polymer blend disc contains only the polymeric compounds and water for the negative control. Petri dishes were incubated in the oven at 37ºC for 24 hours, and the inhibition halos were measured [39].

3. Results and Discussion

3.1. Production of Euterpe oleracea extract and characterization by UV-Vis.

Figure 1 shows the extraction tests for *Euterpe oleracea* extract. The extracts were characterized by UV–Vis in the 200nm - 800nm range. For the production of the extract, green and senescent fruits were used. The ripe fruit route was chosen because, as seen in the spectrum, it presents more intense absorption peaks in the 290 to 690 nm ranges, associated with phenolic compounds and their absorption bands in the ultraviolet. Besides, the peaks are wider and well defined, revealing a more significant amount of extracted compounds and the presence of

antioxidant chemical species. It is worth mentioning that in the route with the ripe fruit, a new band appears, with a peak at 500 nm and a characteristic range of anthocyanins, which may be related to the pH of the medium that was 5 [40].

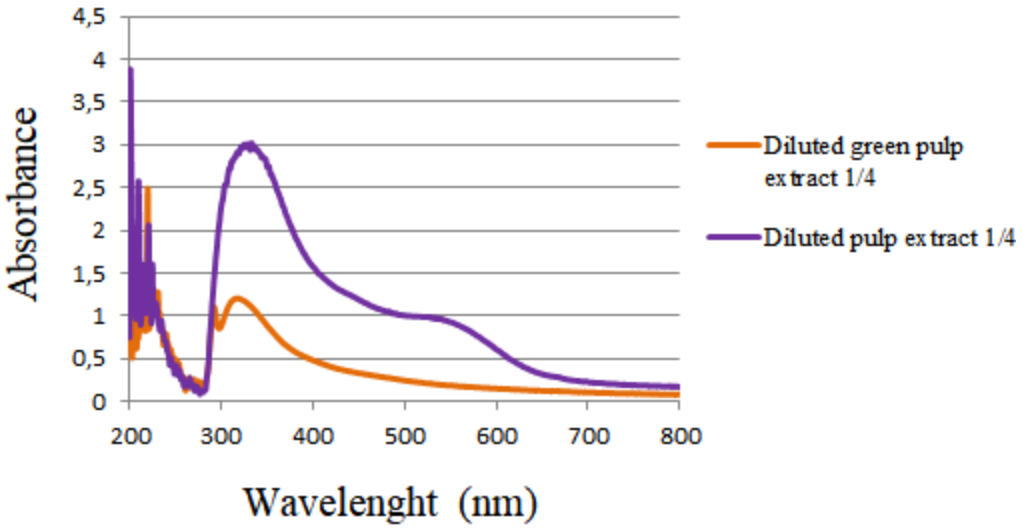

Figure 1. Overlapping UV-Vis analyses of different crops of *Euterpe oleracea* extract.

3.2. Synthesis of AgNPs through green synthesis methodology and characterization of AgNPs by UV-Vis Spectrophotometry.

Figure 2 lists the results obtained in the different synthesis routes of the AgNPs. The heating for 25 seconds was chosen to standardize the work because its absorbance bands are more intense, and the wavelength is 400 nm [41].

The initial characterization of the AgNPs was performed through the reading made by the UV-Vis spectrophotometer. The literature is already well described for the typical silver nanoparticle band, which varies between 380 nm - 500 nm, due to the Plasmonic Surface Resonance phenomenon (RPS). This effect is strongly related to the size, shape, and state of aggregation of the particles. For example, AgNPs with bands between 380-390 nm generally are associated with sizes between 5 to 10 nm, and as they increase in size, these plasmon bands tend to increase [42].

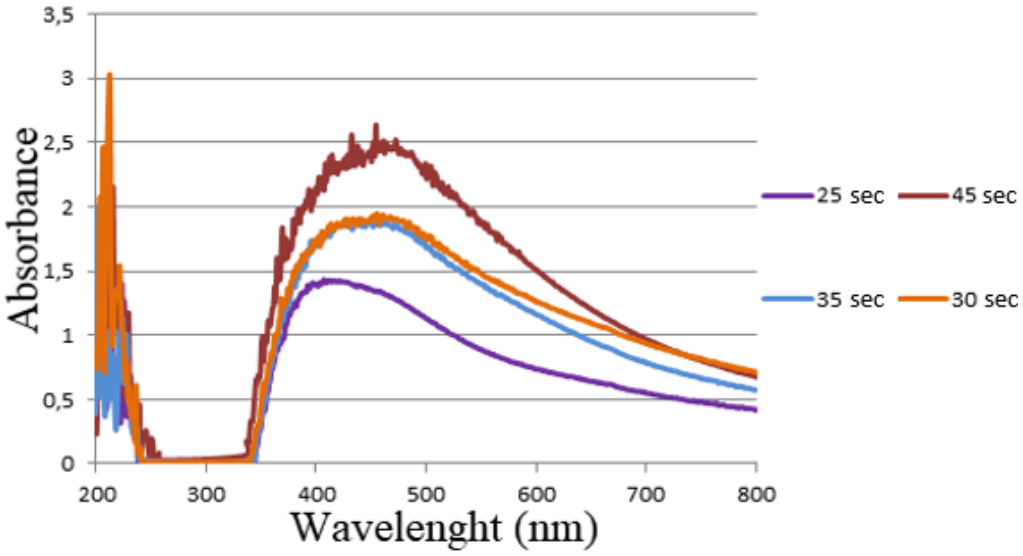

Figure 2. UV-Vis analysis of the green synthesis of AgNPs by different routes and different heating time variations.

3.3. Production of biodegradable film from the polymer blend.

Figure 3 presented the expected morphological pattern, with the preserved starch granules, besides interesting mechanical properties such as good malleability and mechanical resistance. Therefore, polymerized glycerol improved the mechanical properties of the biodegradable film compared to those previously made without increasing it, Figure 4 and 5 [43-45].

Figure 3. Biodegradable film synthesized by an extract with AgNPs.

Figure 4. Biodegradable film.

Figure 5. Polymeric Blend with water.

3.4. Analysis of the film's morphological viability.

Feasibility tests were carried out using biodegradable blends synthesized from *Euterpe oleracea* extract and the AgNPs listed in item 2.7. These tests are intended to macroscopically analyze the film's mechanical strength after surface treatment, using different solutions to treat wounds (Figure 6). In addition, these conditions depend on the exudate (Figure 7). The exact nature of the exudate is associated with the severity of the injury and specific cause. Microscopically, it was possible to analyze if the superficial attack with the different solutions in the blends modified with the AgNPs would change the nanostructures' morphology and dispersion, as shown in Figures VI and VII [46,47]. All samples of blends that were

superficially attacked showed resistance to the solutions and did not show ruptures, an essential factor in producing the nanostructured material.

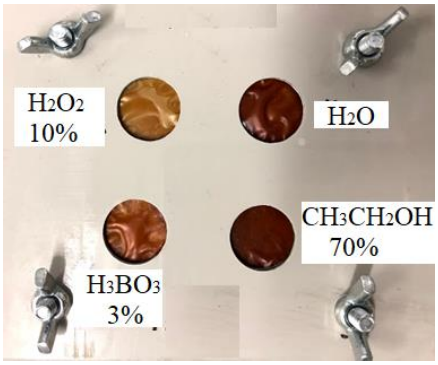

Figure 6. Feasibility test after 24 hours of contact with H_2O, H_2O_2, H_3BO_3, and CH_3CH_2OH.

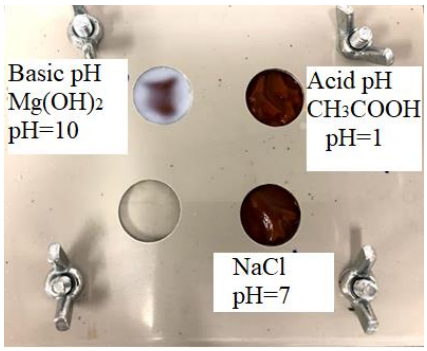

Figure 7. Feasibility test after 24 hours of contact with NaCl, $Mg(OH)_2$, and CH_3COOH solutions.

3.5. Characterization of the biodegradable film with AgNPs by optical microscopy, scanning electron microscopy (SEM), and EDS.

In Figure 8, we have the preliminary characterization of the biodegradable films made based on the extract and impregnated with AgNPs, which were analyzed by optical microscopy with 10x magnification, where analyze the structure of cornstarch. By the result of optical micrographs, we can see the preservation of starch granules [48].

To analyze the presence, dispersion, and behavior of AgNPs, the characterizations by SEM, Figure 9, were made, and to corroborate the micrographs obtained in the SEM, and regarding the existence of AgNPs in the blends, the EDS technique that analyzes the absorption and emission signature of each element on that surface was used, as shown in Figure 10.

Figures 9 (A) and (B) refer to the analysis by SEM and EDS, respectively, where the intention was to analyze whether the dispersive medium of *Euterpe oleracea* was efficient in stabilizing and dispersing AgNPs. Figure 9 (A) shows a micrograph with 200 µm magnification. As a result, it was possible to visualize particles from the AgNPs, visualized as luminous points, characteristic of silver. In Figure 9 (B), we have a micrograph with a 50 µm magnification where we have a better view of the particles coming from the AgNPs. It is important to highlight that the AgNPs are well dispersed throughout the film, which is significant since they do not form clusters in the analyzed images. By EDS, Figure 10, we can confirm the presence of silver in the material since the technique explores each element's absorption and emission. The surface reveals silver's presence, which is the leading study element [49].

Figure 8. Micrograph with 10x magnification of the biodegradable film based on the extract.

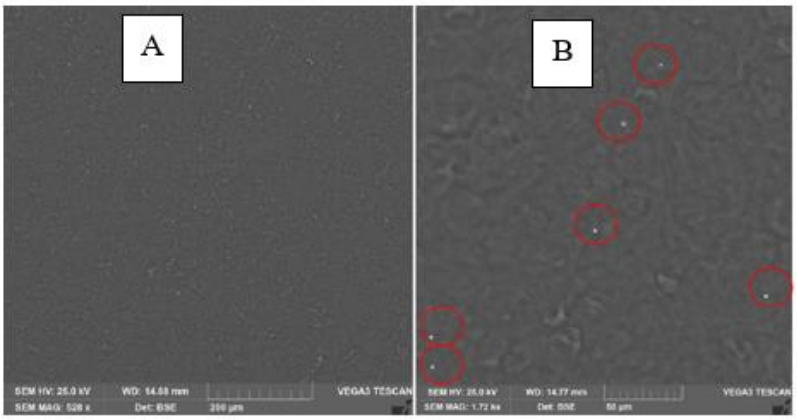

Figure 9. SEM micrographs of film III. In (A) 200 µm magnification and (B) 50 µm magnification with AgNPs marked in red circles.

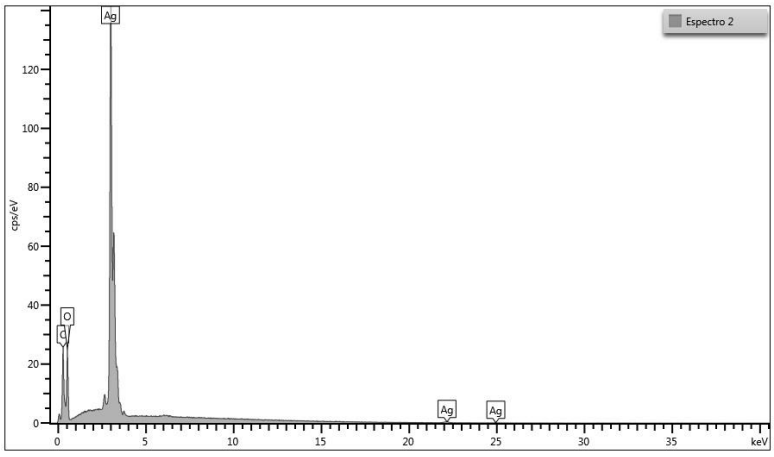

Figure 10. EDS spectrum Ag presence.

3.6. Characterization of AgNPs present in polymer blends after chemical surface treatment by characteristic X-ray mapping.

Figures 11, 12, and 13 show the characteristic X-ray mapping. It was possible to evaluate how the dispersion of the AgNPs, present in the polymeric blend, was current after treatment with a superficial chemical attack. For that, all blends tested with the superficial chemical attack were analyzed by the X-ray mapping technique to verify Ag's presence. This analysis's main purpose was to verify the impact of the superficial chemical treatment on the dispersion of AgNPs in the film. As shown in the Figures below, it was possible to confirm the presence of silver in all treated blends and the preservation of their dispersion. In contrast, the silver was not present in blend I, which was expected because it did not contain $AgNO_3$

insertion; it was just a blend without AgNPs (control). These results are of paramount importance. They make it possible to apply the blends since even in contact with the chemical solutions widely used in injuries in general, the AgNPs presented in the blends do not suffer carrier and aggregation, which would mischaracterize the material as nanostructured [50,51].

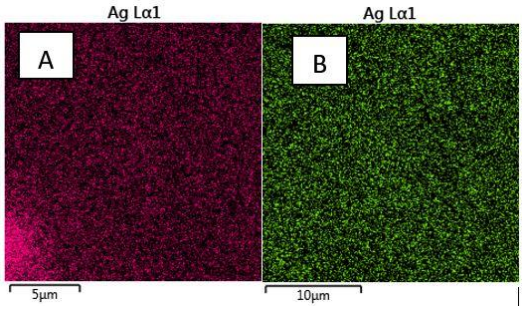

Figure 11. X-ray mapping images of the blend treated with NaCl (A) and CH_3COOH, where the luminous dots represent the presence of Ag (B).

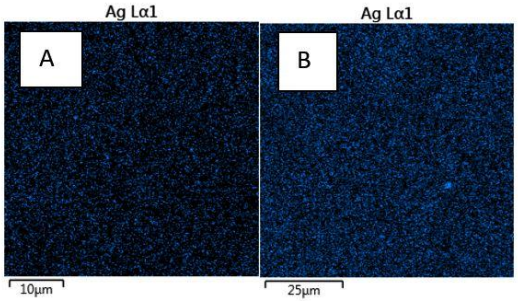

Figure 12. Images of X-ray mapping of the blend treated with $Mg(OH)_2$ (A) and H_2O_2 (B), where the luminous dots represent the presence of Ag.

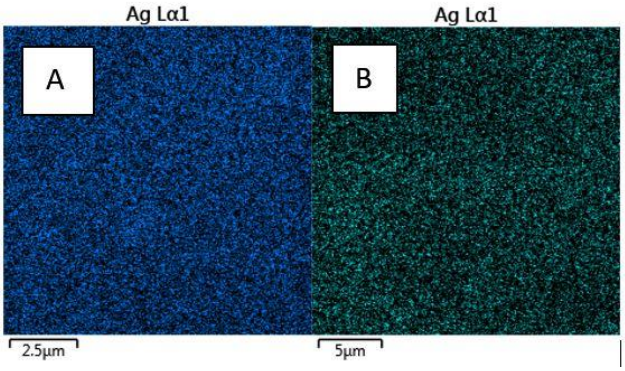

Figure 13. X-ray mapping images of the blend treated with CH_3CH_2OH (A) and H_3BO_3 (B), where the luminous dots represent the presence of Ag.

3.7. Antimicrobial sensitivity test.

After 24 hours on the stove, the results of antimicrobial sensitivity tests were evaluated, as shown in Figure 14. The preliminary results of the qualitative antimicrobial sensitivity test demonstrate that both disks and blends incorporated with silver nitrate and silver nanoparticles have antimicrobial activity against gram-positive strain *S. aureus* ATCC 25923 and concerning the gram-negative strain *E. coli* ATCC 25922. Also, the *Euterpe Oleracea* extract solution with 1:10 diluted AgNPs demonstrated antimicrobial activity when applied to the disc. In contrast, blends and discs incorporated only with water or plant extract did not show antimicrobial activity, except for a slight subinhibitory effect of the extract on *S. aureus* [52–59].

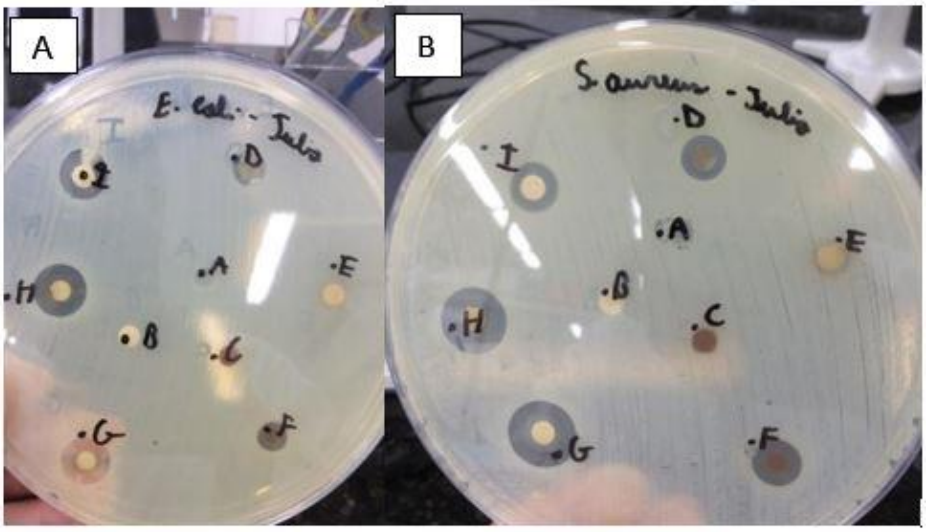

Figure 14. *E. coli* (A) and *S. aureus* (B) antimicrobial sensitivity test.

Table 1. Table with the legend of the tests performed for *E. coli* and *S.aureus* strains.

A – Water-based blend	F – Blend impregnated with AgNPs
B – Empty Disc (negative control)	G – Disc containing the solution of H_2O + $AgNO_3$
C – Extract based blend	H - Disc containing solution of açaí + AgNPs
D – Blend incorporated with $AgNO_3$	I - Disc containing solution of açaí + diluted AgNPs 1:10.
E – Disc with extract	

Table 2. Table with the halos length formed in contact with strains of *E. coli* and *S.aureus.*

E. coli ATCC 25922		*S. aureus* ATCC 25923	
A – No halo formation	F – 9,0 mm	A - No halo formation	F – 11,0 mm
B - No halo formation	G – 14,0 mm	B - No halo formation	G – 17,5 mm
C - No halo formation	H – 15,0 mm	C - No halo formation	H – 17,0 mm
D – 9,0 mm	I – 13,0 mm	D – 10,0 mm	I – 12,0 mm
E - No halo formation		E – Some activity detected	

4. Conclusions

The analyses mede it possível too concluem chat lhe *Euterpe oleracea* extrat. is an efficient, reducing, and stabilizing agent for AgNPs, not being necessary too use toxic compounds for lhe synthesis route of lhe nanoparticles. Furthermore, characterization by UV-Vis, SEM, EDS, and characteristic x-ray mapping confirmed the formation of AgNPs, dispersion, and presence in polymer blends.

The results obtained with the antimicrobial sensitivity test confirmed the efficiency of both the solution with AgNPs (H) and the blend synthesized with AgNPs (F). These results demonstrate the potential of AgNPs as antimicrobials in substitution for silver nitrate, which, even with satisfactory results, has its use, in the long run, as a cause of pathologies such as Argiria's disease. Therefore, the utilization of AgNPs can be an alternative for use in hospital materials and, in the case of blends, for use as wound dressings.

The possibility of using dressings based on biodegradable polymeric films, with excellent adhesion to the skin without the need to use glue and with proven antimicrobial efficiency, innovates the medical field, allowing for better dressing efficiency and low environmental impact.

Funding

This research received no external funding.

Acknowledgments

This research has no acknowledgment.

Conflicts of Interest

The authors declare no conflict of interest.

References

1. Farias, M.G.; Fakhouri, F.M.; Carvalho, C.W.P. de; Ascheri, J.L.R. Caracterização físico-química de filmes comestíveis de amido adicionado de acerola (Malphigia emarginata D.C.). *Quím. Nova* **2012**, *35*, 546–552, https://doi.org/10.1590/S0100-40422012000300020.
2. oste, N.; Chinarro, D.; Gomez, M.; Roldán, E.; Giner, B. Assessing awareness of green chemistry as a tool for advancing sustainability. *Journal of Cleaner Production* **2020**, *256*, https://doi.org/10.1016/j.jclepro.2020.120392.
3. Olaiya, N.G.; Surya, I.; Oke, P.K.; Rizal, S.; Sadiku, E.R.; Ray, S.S.; Farayibi, P.K.; Hossain, M.S.; Abdul Khalil, H.P.S. Properties and Characterization of a PLA–Chitin–Starch Biodegradable Polymer Composite. *Polymers* **2019**, *11*, https://doi.org/10.3390/polym11101656.
4. Karimi, M.; Biria, D. The promiscuous activity of alpha-amylase in biodegradation of low-density polyethylene in a polymer-starch blend. *Scientific Reports* **2019**, *9*, https://doi.org/10.1038/s41598-019-39366-0.
5. Gouveia, T.I.A.; Biernacki, K.; Castro, M.C.R.; Gonçalves, M.P.; Souza, H.K.S. A New Approach to Develop Biodegradable Films Based on Thermoplastic Pectin. *Food Hydrocolloids* **2019,** *97*, https://doi.org/10.1016/j.foodhyd.2019.105175.
6. Pagano, C.; Ceccarini, M.R.; Calarco, P.; Scuota, S.; Conte, C.; Primavilla, S.; Ricci, M.; Perioli, L. Bioadhesive Polymeric Films Based on Usnic Acid for Burn Wound Treatment: Antibacterial and Cytotoxicity Studies. *Colloids Surf B Biointerfaces* **2019**, *178*, 488–499, https://doi.org/10.1016/j.colsurfb.2019.03.001.
7. Bano, I.; Arshad, M.; Yasin, T.; Ghauri, M.A. Preparation, Characterization and Evaluation of Glycerol Plasticized Chitosan/PVA Blends for Burn Wounds. *Int J Biol Macromol* **2019,** *124*, 155–162, https://doi.org/10.1016/j.ijbiomac.2018.11.073.
8. Arthe, R.; Arivuoli, D.; Ravi, V. Preparation and Characterization of Bioactive Silk Fibroin/Paramylon Blend Films for Chronic Wound Healing. *Int J Biol Macromol* **2020**, *154*, 1324–1331, https://doi.org/10.1016/j.ijbiomac.2019.11.010.
9. da Cruz, J.A.; da Silva, A.B.; Ramin, B.B.S.; Souza, P.R.; Popat, K.C.; Zola, R.S.; Kipper, M.J.; Martins, A.F. Poly(Vinyl Alcohol)/Cationic Tannin Blend Films with Antioxidant and Antimicrobial Activities. *Mater Sci Eng C Mater Biol Appl* **2020**, *107*, https://doi.org/10.1016/j.msec.2019.110357.
10. Rosa, D.S.; Franco, B.L.M.; Calil, M.R. Biodegradabilidade e propriedades mecânicas de novas misturas poliméricas. *Polímeros* **2001**, *11*, 82–88, https://doi.org/10.1590/S0104-14282001000200010.
11. Schoch, T.J. The Fractionation of Starch. In: *Advances in Carbohydrate Chemistry*. Pigman, W.W.; Wolfrom, M.L. Eds.; Academic Press, Voulme 1, **1945**; pp. 247–277.
12. Buléon, A.; Colonna, P.; Planchot, V.; Ball, S. Starch Granules: Structure and Biosynthesis. *International Journal of Biological Macromolecules* **1998**, *23*, 85–112, https://doi.org/10.1016/S0141-8130(98)00040-3.
13. Ahmadi, A.; Baker, D.A. The Effect of Water Stress on the Activities of Key Regulatory Enzymes of the Sucrose to Starch Pathway in Wheat. *Plant Growth Regulation* **2001**, *35*, 81–91, https://doi.org/10.1023/A:1013827600528.
14. Jebril, S.; Khanfir Ben Jenana, R.; Dridi, C. Green Synthesis of Silver Nanoparticles Using Melia Azedarach Leaf Extract and Their Antifungal Activities: In Vitro and in Vivo. *Materials Chemistry and Physics* **2020,** *248*, https://doi.org/10.1016/j.matchemphys.2020.122898.
15. Vega-Baudrit, J.; Gamboa, S.M.; Rojas, E.; Martínez, V. Synthesis and Characterization of Silver Nanoparticles and Their Application as an Antibacterial Agent. *International Journal of Biosensors & Bioelectronics* **2019**, *5*, https://doi.org/10.15406/ijbsbe.2019.05.00172.
16. Khan, I.; Saeed, K.; Khan, I. Nanoparticles: Properties, Applications and Toxicities. *Arabian Journal of Chemistry* **2019**, *12*, 908–931, https://doi.org/10.1016/j.arabjc.2017.05.011.
17. Backx, B.P. The Role of Biosynthesized Silver Nanoparticles in Antimicrobial Mechanisms. *Current pharmaceutical biotechnology* **2021,** *22*, 762-772, https://doi.org/10.2174/1389201022666210202143755.

18. Shaik, M.R.; Khan, M.; Kuniyil, M.; Al-Warthan, A.; Alkhathlan, H.Z.; Siddiqui, M.R.H.; Shaik, J.P.; Ahamed, A.; Mahmood, A.; Khan, M.; Adil, S.F. Plant-Extract-Assisted Green Synthesis of Silver Nanoparticles Using Origanum vulgare L. Extract and Their Microbicidal Activities. *Sustainability* **2018**, *10*, https://doi.org/10.3390/su10040913.
19. Sharma, V.; Kaushik, S.; Pandit, P.; Dhull, D.; Yadav, J.P.; Kaushik, S. Green Synthesis of Silver Nanoparticles from Medicinal Plants and Evaluation of Their Antiviral Potential against Chikungunya Virus. *Appl Microbiol Biotechnol* **2019**, *103*, 881–891, https://doi.org/10.1007/s00253-018-9488-1.
20. Garibo, D.; Borbón-Nuñez, H.A.; de León, J.N.D.; García Mendoza, E.; Estrada, I.; Toledano-Magaña, Y.; Tiznado, H.; Ovalle-Marroquin, M.; Soto-Ramos, A.G.; Blanco, A.; Rodríguez, J.A.; Romo, O.A.; Chávez-Almazán, L.A.; Susarrey-Arce, A. Green synthesis of silver nanoparticles using Lysiloma acapulcensis exhibit high-antimicrobial activity. *Scientific Reports* **2020**, *10*, https://doi.org/10.1038/s41598-020-69606-7.
21. Ali, Z.A.; Yahya, R.; Sekaran, S.D.; Puteh, R. Green Synthesis of Silver Nanoparticles Using Apple Extract and Its Antibacterial Properties. *Advances in Materials Science and Engineering* **2016**, *2016*, https://doi.org/10.1155/2016/4102196.
22. Zhang, W.; Jiang, W. Antioxidant and Antibacterial Chitosan Film with Tea Polyphenols-Mediated Green Synthesis Silver Nanoparticle via a Novel One-Pot Method. *Int J Biol Macromol* **2020,** *155*, 1252–1261, https://doi.org/10.1016/j.ijbiomac.2019.11.093.
23. Pelissari, F.M.; Grossmann, M.V.E.; Yamashita, F.; Pineda, E.A.G. Antimicrobial, Mechanical, and Barrier Properties of Cassava Starch−Chitosan Films Incorporated with Oregano Essential Oil. *Journal of Agricultural and Food Chemistry* **2009**, *57*, 7499-7504, https://doi.org/10.1021/jf9002363.
24. Zhang, Q.-W.; Lin, L.-G.; Ye, W.-C. Techniques for Extraction and Isolation of Natural Products: A Comprehensive Review. *Chinese Medicine* **2018**, *13*, https://doi.org/10.1186/s13020-018-0177-x.
25. Trusheva, B.; Trunkova, D.; Bankova, V. Different Extraction Methods of Biologically Active Components from Propolis: A Preliminary Study. *Chemistry Central Journal* **2007**, *1*, https://doi.org/10.1186/1752-153X-1-13.
26. Azwanida, N.N. A review on the extraction methods use in medicinal plants, principle, strength and limitation. *Med Aromat Plants* **2015**, *4*, 2167-0412, http://dx.doi.org/10.4172/2167-0412.1000196.
27. Yahya, N.A.; Attan, N.; Wahab, R.A. An overview of cosmeceutically relevant plant extracts and strategies for extraction of plant-based bioactive compounds. *Food and Bioproducts Processing* **2018**, *112*, 69-85, https://doi.org/10.1016/j.fbp.2018.09.002.
28. Divakaran, D.; Lakkakula, J.R.; Thakur, M.; Kumawat, M.K.; Srivastava, R. Dragon Fruit Extract Capped Gold Nanoparticles: Synthesis and Their Differential Cytotoxicity Effect on Breast Cancer Cells. *Materials Letters* **2019**, *236*, 498–502, https://doi.org/10.1016/j.matlet.2018.10.156.
29. Brindhadevi, K.; Samuel, M.S.; Verma, T.N.; Vasantharaj, S.; Sathiyavimal, S.; Saravanan, M.; Pugazhendhi, A.; Duc, P.A. Zinc oxide nanoparticles (ZnONPs) -induced antioxidants and photocatalytic degradation activity from hybrid grape pulp extract (HGPE). *Biocatalysis and Agricultural Biotechnology* **2020**, *28*, https://doi.org/10.1016/j.bcab.2020.101730.
30. Owaid, M.N. Green Synthesis of Silver Nanoparticles by Pleurotus (Oyster Mushroom) and Their Bioactivity: Review. *Environmental Nanotechnology, Monitoring & Management* **2019**, *12*, https://doi.org/10.1016/j.enmm.2019.100256.
31. Jorge de Souza, T.A.; Rosa Souza, L.R.; Franchi, L.P. Silver Nanoparticles: An Integrated View of Green Synthesis Methods, Transformation in the Environment, and Toxicity. *Ecotoxicol Environ Saf* **2019**, *171*, 691–700, https://doi.org/10.1016/j.ecoenv.2018.12.095.
32. Backx, B.P. Nanobiotechnology and supramolecular mechanistic interactions on approach for silver nanoparticles for healthcare materials. In: *Nanostructures for Antimicrobial and Antibiofilm Applications*. Springer, Cham: **2020**; pp. 185-207.
33. Mohseni, M.S.; Khalilzadeh, M.A.; Mohseni, M.; Hargalani, F.Z.; Getso, M.I.; Raissi, V.; Raiesi, O. Green Synthesis of Ag Nanoparticles from Pomegranate Seeds Extract and Synthesis of Ag-Starch Nanocomposite and Characterization of Mechanical Properties of the Films. *Biocatalysis and Agricultural Biotechnology* **2020,** *25*, https://doi.org/10.1016/j.bcab.2020.101569.
34. Rahimi, M.; Noruzi, E.B.; Sheykhsaran, E.; Ebadi, B.; Kariminezhad, Z.; Molaparast, M.; Mehrabani, M.G.; Mehramouz, B.; Yousefi, M.; Ahmadi, R.; Yousefi, B.; Ganbarov, K.; Kamounah, F.S.; Shafiei-Irannejad, V.; Kafil, H.S. Carbohydrate polymer-based silver nanocomposites: Recent progress in the antimicrobial wound dressings. *Carbohydrate Polymers* **2020**, *231*, https://doi.org/10.1016/j.carbpol.2019.115696.
35. Adeli, H.; Khorasani, M.T.; Parvazinia, M. Wound Dressing Based on Electrospun PVA/Chitosan/Starch Nanofibrous Mats: Fabrication, Antibacterial and Cytocompatibility Evaluation and in Vitro Healing Assay. *Int J Biol Macromol* **2019**, *122*, 238–254, https://doi.org/10.1016/j.ijbiomac.2018.10.115.
36. Rana, A.; Yadav, K.; Jagadevan, S. A Comprehensive Review on Green Synthesis of Nature-Inspired Metal Nanoparticles: Mechanism, Application and Toxicity. *Journal of Cleaner Production* **2020**, *272*, https://doi.org/10.1016/j.jclepro.2020.122880.
37. Jenifer, A.A.; Malaikozhundan, B.; Vijayakumar, S.; Anjugam, M.; Iswarya, A.; Vaseeharan, B. Green Synthesis and Characterization of Silver Nanoparticles (AgNPs) Using Leaf Extract of Solanum nigrum and

Assessment of Toxicity in Vertebrate and Invertebrate Aquatic Animals. *Journal of Cluster Science* **2020**, *31*, 989-1002, https://doi.org/10.1007/s10876-019-01704-7.
38. Ponsanti, K.; Tangnorawich, B.; Ngernyuang, N.; Pechyen, C. A Flower Shape-Green Synthesis and Characterization of Silver Nanoparticles (AgNPs) with Different Starch as a Reducing Agent. *Journal of Materials Research and Technology* **2020**, *9*, 11003–11012, https://doi.org/10.1016/j.jmrt.2020.07.077.
39. Backx, B.P.; Delazare, T. The influence of dispersive medium on efficient and eco-friendly synthesis of silver nanoparticles for application in antimicrobial fabric. *Revista Verde de Agroecologia e Desenvolvimento Sustentável* **2019**, *14*, 252–257, https://doi.org/10.18378/rvads.v14i2.6163.
40. Uddin, A.K.M.R.; Siddique, Md.A.B.; Rahman, F.; Ullah, A.K.M.A.; Khan, R. Cocos Nucifera Leaf Extract Mediated Green Synthesis of Silver Nanoparticles for Enhanced Antibacterial Activity. *J Inorg Organomet Polym* **2020**, *30*, 3305–3316, https://doi.org/10.1007/s10904-020-01506-9.
41. Santos, M.S. dos; Backx, B.P. Factors that influence the stability of silver nanoparticles dispersed in propolis. *ACTA Apicola Brasilica* **2020**, *8*, https://doi.org/10.18378/aab.v8i0.7805.
42. Sridhara, V.; Pratima, K.; Krishnamurthy, G.; Sreekanth, B. Vegetable assisted synthesis of silver nanoparticles and its antibacterial activity against two human pathogens. *Acharya Institutes* **2013**.
43. Rezende, D.J.L.F.d.; Sarrouh, B.; Naves, F.L.; Lofrano, R.C.Z. Uso de glicerina residual e glicerol na preparação de biopolímero. *Revista Eletrônica em Gestão, Educação e Tecnologia Ambiental* **2019**, *23*, https://doi.org/10.5902/2236117034859.
44. Lavorgna, M.; Piscitelli, F.; Mangiacapra, P.; Buonocore, G. Study of the combined effect of both clay and glycerol plasticizer on the properties of chitosan films. *Carbohydrate Polymers* **2010**, *82*, 291-298, https://doi.org/10.1016/j.carbpol.2010.04.054.
45. Esmaeili, M.; Pircheraghi, G.; Bagheri, R. Optimizing the mechanical and physical properties of thermoplastic starch via tuning the molecular microstructure through co-plasticization by sorbitol and glycerol. *Polymer International* **2017**, *66*, 809-819, https://doi.org/10.1002/pi.5319.
46. Yang, X.; Liu, W.; Xi, G.; Wang, M.; Liang, B.; Shi, Y.; Feng, Y.; Ren, X.; Shi, C. Fabricating Antimicrobial Peptide-Immobilized Starch Sponges for Hemorrhage Control and Antibacterial Treatment. *Carbohydrate Polymers* **2019**, *222*, https://doi.org/10.1016/j.carbpol.2019.115012.
47. Movahedi, M.; Asefnejad, A.; Rafienia, M.; Khorasani, M.T. Potential of Novel Electrospun Core-Shell Structured Polyurethane/Starch (Hyaluronic Acid) Nanofibers for Skin Tissue Engineering: In Vitro and in Vivo Evaluation. *International Journal of Biological Macromolecules* **2020,** *146*, 627–637, https://doi.org/10.1016/j.ijbiomac.2019.11.233.
48. Abdullah, O.Gh.; Hanna, R.R.; Salman, Y.A.K. Structural, Optical, and Electrical Characterization of Chitosan: Methylcellulose Polymer Blends Based Film. *J Mater Sci: Mater Electron* **2017**, *28*, 10283–10294, https://doi.org/10.1007/s10854-017-6796-7.
49. Hashim, A.; Hadi, Q. Structural, Electrical and Optical Properties of (Biopolymer Blend/Titanium Carbide) Nanocomposites for Low Cost Humidity Sensors. *J Mater Sci: Mater Electron* **2018,** *29*, 11598–11604, https://doi.org/10.1007/s10854-018-9257-z.
50. Lawrie, G.; Keen, I.; Drew, B.; Chandler-Temple, A.; Rintoul, L.; Fredericks, P.; Grøndahl, L. Interactions between Alginate and Chitosan Biopolymers Characterized Using FTIR and XPS. *Biomacromolecules* **2007**, *8*, 2533–2541, https://doi.org/10.1021/bm070014y.
51. Monisha, S.; Mathavan, T.; Selvasekarapandian, S.; Benial, A.M.F.; latha, M.P. Preparation and Characterization of Cellulose Acetate and Lithium Nitrate for Advanced Electrochemical Devices. *Ionics* **2017**, *23*, 2697–2706, https://doi.org/10.1007/s11581-016-1886-8.
52. Ribeiro, G.S. Síntese de nanopartículas de prata mediada por extratos aquosos de Euterpe oleracea (açaí). *Instituto de Ciências Exatas e Tecnologia* **2019**.
53. Aadil, K.R.; Pandey, N.; Mussatto, S.I.; Jha, H. Green Synthesis of Silver Nanoparticles Using Acacia Lignin, Their Cytotoxicity, Catalytic, Metal Ion Sensing Capability and Antibacterial Activity. *Journal of Environmental Chemical Engineering* **2019**, *7*, https://doi.org/10.1016/j.jece.2019.103296.
54. Mariadoss, A.V.A.; Ramachandran, V.; Shalini, V.; Agilan, B.; Franklin, J.H.; Sanjay, K.; Alaa, Y.G.; Tawfiq, M.A.; Ernest, D. Green synthesis, characterization and antibacterial activity of silver nanoparticles by Malus domestica and its cytotoxic effect on (MCF-7) cell line. *Microbial pathogenesis* **2019**, *135*, https://doi.org/10.1016/j.micpath.2019.103609.
55. Anandan, M.; Poorani, G.; Boomi, P.; Varunkumar, K.; Anand, K.; Chuturgoon, A.A.; Saravanan, M.; Gurumallesh Prabu, H. Green synthesis of anisotropic silver nanoparticles from the aqueous leaf extract of Dodonaea viscosa with their antibacterial and anticancer activities. *Process Biochemistry* **2019**, *80*, 80-88, https://doi.org/10.1016/j.procbio.2019.02.014.
56. Zhu, M.; Li, X.; Ge, L.; Zi, Y.; Qi, M.; Li, Y.; Li, D.; Mu, C. Green Synthesis of κ-Carrageenan@Ag Submicron-Particles with High Aqueous Stability, Robust Antibacterial Activity and Low Cytotoxicity. *Mater Sci Eng C Mater Biol Appl* **2020**, *106*, https://doi.org/10.1016/j.msec.2019.110185.
57. Nouri, A.; Tavakkoli Yaraki, M.; Lajevardi, A.; Rezaei, Z.; Ghorbanpour, M.; Tanzifi, M. Ultrasonic-Assisted Green Synthesis of Silver Nanoparticles Using Mentha Aquatica Leaf Extract for Enhanced Antibacterial Properties and Catalytic Activity. *Colloid and Interface Science Communications* **2020**, *35*, https://doi.org/10.1016/j.colcom.2020.100252.

58. Morales-Lozoya, V.; Espinoza-Gómez, H.; Z. Flores-López, L.; Sotelo-Barrera, E.L.; Núñez-Rivera, A.; Cadena-Nava, R.D.; Alonso-Nuñez, G.; Rivero, I.A. Study of the Effect of the Different Parts of Morinda Citrifolia L. (Noni) on the Green Synthesis of Silver Nanoparticles and Their Antibacterial Activity. *Applied Surface Science* **2021**, *537*, https://doi.org/10.1016/j.apsusc.2020.147855.
59. Mogoşanu, G.D.; Grumezescu, A.M. Natural and Synthetic Polymers for Wounds and Burns Dressing. *International Journal of Pharmaceutics* **2014,** *463*, 127–136, https://doi.org/10.1016/j.ijpharm.2013.12.015.